Editors' Suggestion

Localized $AdS_3 \times S^3 \times T^4$ Black Holes

Óscar J. C. Dias[1,*] and Jorge E. Santos[2,†]
[1]STAG Research Centre and Mathematical Sciences, University of Southampton, Southampton SO17 1BJ, United Kingdom
[2]Department of Applied Mathematics and Theoretical Physics, University of Cambridge, Wilberforce Road, Cambridge CB3 0WA, United Kingdom

(Received 22 September 2025; accepted 8 December 2025; published 20 January 2026)

We numerically construct asymptotically global $AdS_3 \times S^3 \times T^4$ black holes in type IIB supergravity, with $\mathbb{R}_t \times SO(2) \times SO(3) \times U(1)^4$ symmetry, localized on the S^3 and translationally invariant along the torus. These solutions, with horizons whose spatial cross sections have $S^4 \times T^4$ topology, dominate the microcanonical ensemble at low energies. At higher energies, a first-order phase transition occurs to BTZ $\times$ $S^3 \times T^4$ black holes—possessing $\mathbb{R}_t \times SO(2) \times SO(4) \times U(1)^4$ symmetry and $S^1 \times S^3 \times T^4$ horizon topology. By the AdS/CFT correspondence, this transition reflects the spontaneous breaking of the SO(4) R symmetry of the $D1$-$D5$ CFT_2 to SO(3). We also compute the expectation value of the scalar operator with lowest conformal dimension in the low-energy phase. Our SO(3)-localized black holes—together with the $U(1)^2$-localized solutions of Bena *et al.* [J. High Energy Phys. 10 (2025) 165.]—point to a rich landscape of novel black holes that may approach the CFT_2 "sparseness bootstrap condition," and shed light on how macroscopic entanglement in thermal phases encodes microscopic structure via internal directions.

DOI: 10.1103/f2rs-p1mq

Introduction—AdS/CFT correspondence is the prototypical example of a holographic duality [1–3] and remains a key tool for studying strongly coupled physics and quantum gravity. In particular, $D1-D5$ CFT_2/AdS_3 duality provides a solvable test bed for exploring holography [4,5]. On one side, the $D1-D5$ CFT_2, a two-dimensional $\mathcal{N}=(4,4)$ superconformal field theory, is among the simplest conformal field theories (CFTs). On the other, $AdS_3 \times X$ gravity (with X a compact manifold) is notably tractable—within pure gravity with global AdS_3 asymptotics, the Bañados-Teitelboim-Zanelli (BTZ) black hole is unique. When embedded in type IIB supergravity with $AdS_3 \times S^3 \times T^4$ asymptotics, the BTZ $\times$ $S^3 \times T^4$ black hole (with sufficiently large temperature T) is dual to thermal states in the gauge theory on $\mathbb{R}_t \times S^1$, with the same T [6]. Within this symmetry class, the type IIB equations of motion require the S^3 radius L to match the AdS_3 length scale. These black holes preserve $\mathbb{R}_t \times SO(2) \times SO(4) \times U(1)^4$ symmetry and we shall henceforth refer to this phase simply as the BTZ, or uniform, phase. However, they only exist for energies $E/N^2 > 0$, while the dual CFT_2 has thermal states for $E > -(c/12)$, with $c = 6N^2$ the central charge. Hence, corresponding black holes should exist all the way down to $E = -(c/12)$.

This puzzle was partly resolved by [7], which analyzed novel $AdS_3 \times S^3 \times T^4$ black holes breaking SO(4) symmetry to $U(1)^2$—the so-called "$U(1)^2$ localized black holes" or "black poles" [8]. These exist for $-(c/12) < E \leq (c/96)$ and dominate the microcanonical ensemble for $-(c/12) < E < (c/24)(5\sqrt{5}-11)$, partially overlapping with BTZ.

The existence of these $U(1)^2$ localized black holes hints at another class—those localized on S^3, breaking SO(4) down to SO(3). Such "SO(3) localized black holes" would be more symmetric than the $U(1)^2$ black poles, suggesting they should possess higher entropy at fixed energy. Unlike BTZ black holes and black poles—both with horizons whose spatial cross sections have $S^1 \times S^3 \times T^4$ topology [11]—SO(3) localized black holes would have horizons with $S^4 \times T^4$ spatial cross sections.

One might expect SO(3) localized black holes to exist by analogy with $SO(n)$-symmetric black holes in asymptotically $AdS_k \times S^n$ spacetimes [12–15], where the uniform phase becomes unstable to localization via the Gregory-Laflamme mechanism [16–22]. However, we find that the uniform SO(4) phase—the BTZ $\times$ $S^3 \times T^4$ black hole—is not Gregory-Laflamme unstable. From this perspective, one might expect SO(3) localized black holes not to exist.

Nevertheless, we were motivated to search for them, as the $S^4 \times T^4$ topology of the spatial cross sections of their horizon suggests they should appear pointlike on S^3 at low E/c, effectively behaving as six-dimensional spherical

*Contact author: ojcd1r13@soton.ac.uk
†Contact author: jss55@cam.ac.uk

Published by the American Physical Society under the terms of the Creative Commons Attribution 4.0 International license. Further distribution of this work must maintain attribution to the author(s) and the published article's title, journal citation, and DOI. Funded by SCOAP³.

black holes with the torus as a spectator. Their entropy should scale as $S \sim (E + c/12)^{4/3}$, compared to $S \sim (E + c/12)^{3/2}$ for the $U(1)^2$ black poles [7], suggesting higher entropy at small energies. They should therefore dominate up to a critical energy, beyond which a first-order phase transition to either the BTZ black hole or a black pole may occur. By AdS/CFT, S^3 symmetries correspond to R symmetries in the $D1-D5$ CFT_2, so black holes breaking these symmetries are dual to thermal states with spontaneously broken R symmetry (and nonzero scalar expectation values). This transition interpolates between symmetric thermal states at high energies and symmetry-breaking phases at low energies.

In this Letter, we numerically construct SO(3) localized black holes and prove their existence. They always dominate over the $U(1)^2$ black poles of [7] in the microcanonical ensemble. We also find they entropically dominate over the uniform phase (i.e., BTZ black hole) at low energies, determine the critical point of the first-order phase transition, and compute the expectation value of a scalar operator in the dual field theory. Via the duality, our results yield new quantitative predictions for the $D1-D5$ CFT_2.

Problem setup—We focus on asymptotically $AdS_3 \times S^3 \times T^4$ solutions in type IIB supergravity. The bosonic sector of type IIB supergravity can be succinctly described by the ten-dimensional metric g_{10D}, the complex axion-dilaton field $\tau = C_0 + ie^{-\phi}$, a self-dual five-form field strength $F_{(5)}$, and a complex three-form field strength $G_{(3)}$. We restrict attention to solutions where the axion-dilaton τ and the five-form field strength $F_{(5)}$ vanish. The ten-dimensional metric then takes the form

$$ds^2_{10D} = ds^2_{6D} + ds^2_{T^4}, \tag{1}$$

while the complex three-form field strength reduces to a Ramond-Ramond three-form that is self-dual with respect to the six-dimensional metric, i.e., $G_{(3)} = F_{(3)} =_6 \star F_{(3)}$. The vanishing dilaton, together with the self-duality of $F_{(3)}$, ensures that the numbers of $D1$ (N_1) and $D5$ (N_5) branes coincide, so that the central charge of the corresponding field theory is simply $c = 6N_1N_5 = 6N^2$ [23]. Under these assumptions, the type IIB equations of motion reduce to

$$E_{MN} \equiv R_{MN} - \frac{1}{4} F_{(3)\,MPQ} F_{(3)\,N}{}^{PQ} = 0,$$
$$dF_{(3)} = 0, \qquad F_{(3)} =_6 \star F_{(3)}, \tag{2}$$

with uppercase Latin indices running over the six-dimensional spacetime. We seek static black hole solutions with topology $S^4 \times T^4$. Among these, the most symmetric configurations are expected to maximize the entropy. Such solutions exhibit $\mathbb{R}_t \times SO(2) \times SO(3) \times U(1)^4$ symmetry, preserving the full SO(2) isometry of AdS_3 together with the largest subgroup of SO(4).

We employ the DeTurck method [21,22,24], which requires choosing a reference metric $\bar{g}$ that shares the symmetries and causal structure of the target solution. We choose the reference metric

$$\overline{ds}^2 = \frac{L^2}{(1-y^2)^2}\left\{-H_1 dt^2 + H_2\left[\frac{4dy^2}{2-y^2} + y^2(2-y^2)d\phi^2\right]\right\} + L^2 H_2\left[\frac{16dx^2}{2-x^2} + 4x^2(2-x^2)(1-x^2)^2 d\Omega_2^2\right], \tag{3}$$

where H_1, H_2 are judiciously chosen functions. Specifically, when $H_1 = H_2 = 1$, the metric reduces to global $AdS_3 \times S^3$. Consequently, we require that H_1 and H_2 approach 1 as $y \to 1$ to recover this asymptotic geometry. Additionally, H_1 and H_2 must be chosen so that the reference metric describes a regular S^4 black hole. In fact, for small black holes, the geometry near the horizon is expected to approximate the six-dimensional asymptotically flat Schwarzschild solution ($Schw_6$).

To ensure that H_1 and H_2 satisfy these requirements, we apply the following coordinate transformations. First, we define $y = \sqrt{1 - \mathrm{sech}(Y)}$ and $x = \sqrt{1 - \sin(X/2)}$, which map the dx^2 and dy^2 components of the reference metric to $L^2 H_2(dX^2 + dY^2)$, a form that is conformal to Cartesian coordinates. Finally, setting $X = \rho\xi\sqrt{2-\xi^2}$ and $Y = \rho(1-\xi^2)$ defines a transformation from Cartesian to polar coordinates using an alternative polar coordinate set $\{\rho, \xi\}$. After the mapping, the DeTurck reference metric (3) becomes

$$\overline{ds}^2 = -M\left(\frac{\rho^3 - \rho_0^3}{\rho^3 + \rho_0^3}\right)^2 dt^2 + L^2 H_2\left\{d\rho^2 + \rho^2\left[\frac{4d\xi^2}{2-\xi^2} + G_1\xi^2(2-\xi^2)d\phi^2 + G_2(1-\xi^2)^2 d\Omega_2^2\right]\right\}, \tag{4}$$

where the map $\{x, y\} = \{x(\rho, \xi), y(\rho, \xi)\}$ uniquely determines G_1 and G_2, and relates M directly with H_1. In the dt^2 component, the factor $(\rho^3 - \rho_0^3)^2/(\rho^3 + \rho_0^3)^2$ is included to anticipate the placement of a black hole horizon in the reference metric. We set $H_2 = (1 + \rho_0^3/\rho^3)^{4/3}$, which satisfies the requirement that $H_2 \to 1$ as $y \to 1$ ($\rho \to \infty$). For small ρ and ρ_0, we have $G_1 \approx G_2 \approx 1$, so if $M \approx 1$, the reference metric approximates $Schw_6$ in isotropic coordinates. This behavior guides our choice of H_1, and consequently of M and G_3. We choose H_1 so that $H_1 = 1$ at $y \to 1$ ($\rho \to \infty$) and M is positive definite with $M = 1$ at $\rho = \rho_0$. This condition also fixes the temperature and ensures the regularity of the horizon. Explicit expressions for these functions are provided in Supplemental Material [25].

Given a reference metric $\bar{g}$, the DeTurck method transforms the Einstein equation (2) into

$$E_{MN} - \nabla_{(M}\xi_{N)} = 0, \qquad \xi^M \equiv g^{PQ}[\Gamma^M_{PQ} - \bar{\Gamma}^M_{PQ}], \quad (5)$$

where Γ^M_{PQ} and $\bar{\Gamma}^M_{PQ}$ define the Levi-Civita connections for g and $\bar{g}$, respectively. Unlike (2), this formulation yields partial differential equations (PDEs) that are elliptic in nature. After solving these equations, we must check that $\xi^M = 0$ to ensure that (2) is satisfied. The local uniqueness of elliptic equations guarantees that solutions with $\xi^M = 0$ are distinct from those with $\xi^M \neq 0$. Moreover, the condition $\xi^M = 0$ completely fixes the coordinate freedom in the metric.

We adopt a general ansatz consistent with the symmetries, with the metric depending on six arbitrary functions to be determined numerically. We now turn our attention to $F_{(3)}$. Locally, the three-form field strength $F_{(3)}$ can be expressed in terms of a two-form potential $C_{(2)}$ as $F_{(3)} = \mathrm{d}C_{(2)}$, since $\mathrm{d}F_{(3)} = 0$. The gauge potential $C_{(2)}$ takes the form

$$C_{(2)} = L^2 F \mathrm{d}t \wedge \mathrm{d}\phi + L^2 W \mathrm{Vol}_{\Omega_2}, \quad (6)$$

where F and W are unknown functions, and Vol_{Ω_2} is the volume form on S^2. Applying the self-duality condition together with the Bianchi identity for $F_{(3)}$ leads to a single second-order PDE for F, which allows W to be fully determined in terms of F and its derivatives, and thus eliminated from all the equations of motion.

Our integration domain contains five boundaries: the horizon $\rho = \rho_0$, asymptotic infinity $y = 1$ ($\rho \to \infty$), the S^1 axis $y = 0$ ($\xi = 0$), the S^3 "north" pole $x = 1$ ($\xi = 1$), and the "south" pole $x = 0$. At infinity, as a boundary condition, we impose global $AdS_3 \times S^3$ asymptotics. Regularity determines the remaining boundary conditions (details in Supplemental Material [25]).

To handle the five boundaries numerically, we divide the integration domain into six warped rectangular "patches" (see Supplemental Material [25]). The four patches I–IV far from the horizon use $\{x, y\}$ coordinates, while the remaining two patches V–VI use $\{\rho, \xi\}$ coordinates. We require that the metric g, the form $C_{(2)}$, and their first derivatives match across patch boundaries.

We therefore have a boundary value problem for seven functions of two variables. L drops out of the equations of motion, so the only parameter is ρ_0 which fixes the temperature [26]. We solve the system using a Newton-Raphson algorithm, starting from the reference metric and $F = 1$ at $\rho_0 = 0.1$ as the initial seed. Pseudospectral collocation is employed, with transfinite interpolation of Chebyshev grids in each patch, and the resulting linear systems are solved via LU decomposition. All solutions satisfy $\xi^2 < 10^{-10}$. Further details, including explicit expressions for our ansatz and numerical convergence tests, are provided in Supplemental Material [25] (see also Ref. [22]).

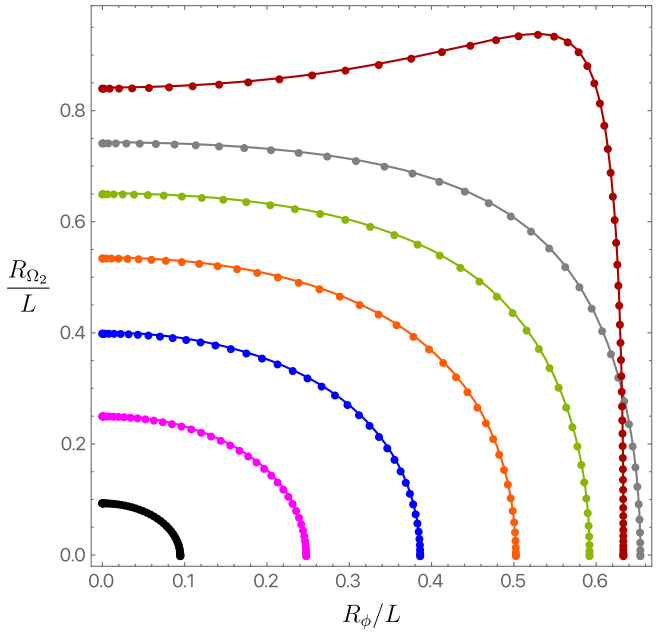


FIG. 1. Radii of the S^1 and S^2 (in units of L) along the horizon. From bottom left to top right the curves have $TL \approx \{2.507, 0.940, 0.578, 0.418, 0.327, 0.269, 0.123\}$.

Results—Figure 1 presents a parametric plot of the radii R_ϕ and R_{Ω_2} of the geometrically preserved S^1 and S^2 along the horizon. For small ρ_0 (high temperatures), the curve is well approximated by $R_\phi^2 + R_{\Omega_2}^2 \approx 2^{4/3}\rho_0^2 L^2$, indicating that the horizon is nearly spherical. As ρ_0 increases (lower temperatures), the horizon becomes significantly more deformed.

We now compute the thermodynamic quantities. The temperature T is determined by ρ_0, while the entropy S is obtained by integrating the horizon area. The energy E is calculated using either the Kaluza-Klein holographic renormalization formalism [27,28] (see also Refs. [12,29–36]) or the covariant Noether charge (covariant phase) method [37–42] (see also Supplemental Material [25]). In the AdS/CFT dictionary, the six- and three-dimensional Newton constants are related to the central charge of the dual CFT_2 via $G_6 = (\pi^2/2)(L^4/N^2)$ and $G_3 = (G_6/2\pi^2 L^3)$. Numerically, these thermodynamic quantities satisfy the first law, $\mathrm{d}E = T, \mathrm{d}S$, to better than 0.1% accuracy.

In the microcanonical ensemble, the energy is fixed, and the dominant solution is the one that maximizes the entropy. Figure 2 shows S/N^2 versus EL/N^2 for various competing solutions. At low energies, the entropy of the SO(3)-localized black hole (blue disks) is well approximated by that of $Schw_6 \times T^4$ (dashed red curve; hereafter, we restore the spectator torus). When both solutions

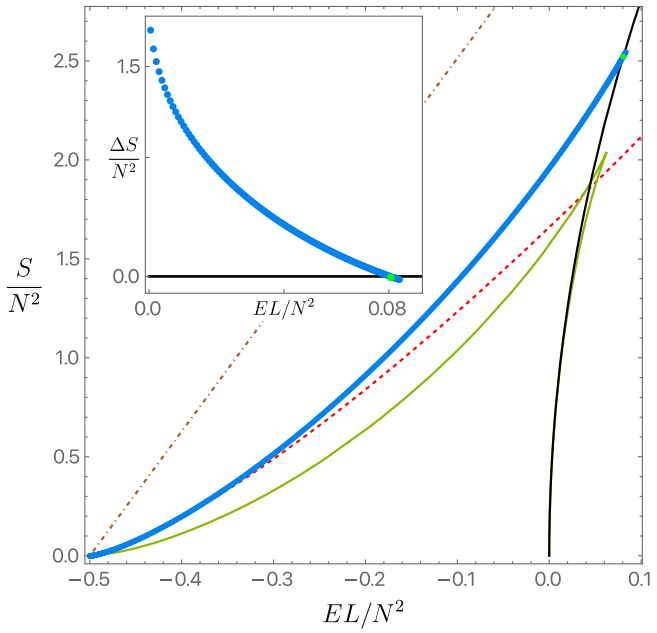


FIG. 2. Microcanonical phase diagram: entropy vs energy. The black line is the BTZ $\times$ S^3 $\times$ T^4 phase, the green curve is the $U(1)^2$ localized phase [7] and the blue dots are the SO(3) localized phase. The red dashed line is the lowest-order Schw$_6$ $\times$ T^4 approximation and the dot-dashed brown line is the "sparseness" bound.

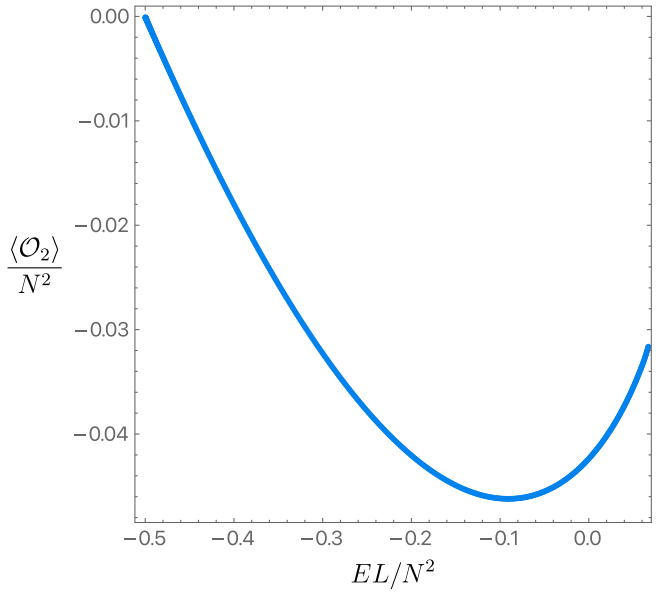


FIG. 3. Dimension 2 scalar condensate vs energy.

coexist, starting at $EL/N^2 = -1/2$, the SO(3)-localized black holes always have higher entropy than the $U(1)^2$-localized solutions of [7] (green curve). The inset plot shows the entropy of the SO(3)-localized solutions relative to that of BTZ $\times$ S^3 $\times$ T^4 (continuous black curve) in the coexistence region. For energies $-\frac{1}{2}(N^2/L) \leq E < E_c$, the SO(3)-localized black holes remain the phase with the highest entropy, exceeding even that of BTZ $\times$ S^3 $\times$ T^4. At the critical energy $E_c L/N^2 \approx 0.0804 \pm 0.0002$ (with $S_c/N^2 \approx 2.52216 \pm 0.0002$, indicated by the green point), a first-order phase transition occurs: above E_c, the BTZ $\times$ S^3 $\times$ T^4 solution dominates the microcanonical ensemble, having the highest entropy.

Returning to the discussion in the Introduction, we note that, unlike the uniform solutions in other $AdS_k \times S^n$ systems (e.g., $AdS_5 \times S^5$ [12–15,43–45]), we find that BTZ $\times$ S^3 $\times$ T^4 is *not* unstable to a Gregory-Laflamme–type instability at any energy. Remarkably, this does not rule out the existence of SO(3)-localized solutions. However, it does exclude the existence of "lumpy" black holes—solutions with horizon topology $S^1 \times S^3 \times T^4$ that are deformed along the polar direction of S^3—which are perturbatively close to BTZ. Such lumpy black holes do exist in the $AdS_5 \times S^5$ system [12–15].

To see this explicitly, we consider linear perturbations of BTZ $\times$ S^3 $\times$ T^4 at temperature T. We perform a Fourier decomposition $e^{-i\omega t}$ along the time direction t and a harmonic decomposition on the S^2, expanding all perturbations in terms of the standard spherical harmonics $Y_{\ell m}$ with $\ell \in \mathbb{Z}^+$ and $|m| \leq \ell$. Solving the resulting eigenvalue problem, we find (details to be presented elsewhere) that the frequencies are quantized as

$$\omega = -2\pi T(2 + 2p + \ell)i, \tag{7}$$

where $p \in \mathbb{Z}^+$ is a radial overtone. Since these frequencies always have a negative imaginary part, there is no Gregory-Laflamme instability.

As noted in the Introduction, localized black holes are dual to thermal states in which the R symmetry of the $D1$-$D5$ CFT_2 is spontaneously broken, in our case down to SO(3). This breaking triggers the condensation of an infinite tower of scalar operators with increasing conformal dimension Δ, the lowest of which has dimension 2. The expectation value $\langle \mathcal{O}_2 \rangle$ of this operator in the broken phase can be computed using the formalism of Kaluza-Klein holography [27,28] (see Supplemental Material [25]). Figure 3 shows $\langle \mathcal{O}_2 \rangle$ across a range of energies. Because the symmetry-breaking transition is first order, $\langle \mathcal{O}_2 \rangle$ takes a nonzero value at the phase transition.

In the canonical ensemble, the temperature is fixed, and the solution with the lowest free energy $F = E - TS$ dominates. In this ensemble, a first-order Hawking-Page phase transition occurs between thermal $AdS_3 \times S^3 \times T^4$ at low temperatures and BTZ $\times$ S^3 $\times$ T^4 black holes at high temperatures [46,47]. Localized black holes, whether SO(3) or $U(1)^2$, never dominate in this ensemble (see Supplemental Material for a phase diagram [25]).

Discussion—We have numerically constructed asymptotically global $AdS_3 \times S^3 \times T^4$ localized black holes in type IIB supergravity that preserve the largest subgroup

SO(3) of SO(4). These black holes, with horizon topology $S^4 \times T^4$, are more entropic than any other known solutions at low energies, with a first-order transition to BTZ $\times$ $S^3 \times T^4$ black holes near $EL/N^2 \approx 0.0804$. Via AdS/CFT, they are dual to thermal states of the strongly coupled $D1-D5$ CFT_2 with spontaneously broken R symmetry, where the lowest-dimension scalar operator has $\Delta = 2$ and preserves SO(3) (see Fig. 3).

Lattice studies of holographic field theories have focused on the canonical ensemble [48–54], but recent work on first-order transitions in other ensembles [55–57] suggests that the $D1$-$D5$ CFT_2 at large N and strong coupling should reproduce Figs. 2 and 3, providing then a precision holography test.

SO(3) localized solution on the S^3 with two or more black holes like ours should exist (very much like in the original black string setup [58–61]). They should exist even with different local masses but should be dynamically unstable to merging into our single SO(3) localized black hole and thus should have less entropy. Such an infinite set of multiblack hole solutions should fill the area below the blue curve and the black curve (and slightly extend to the right of the latter) in the phase diagram of Fig. 2.

The phase diagram that completes the SO(3)-localized curve in Fig. 2 can be conjectured: analogous to the green $U(1)^2$ solutions, SO(3) black holes likely extend to a maximum energy, forming a lower branch down to $\{E, S\} = \{0, 0\}$ where they meet extremal BTZ $\times S^3 \times T^4$ and extremal $U(1)^2$ holes (see Supplemental Material [25]).

Modular bootstrap constraints on large-c CFTs [7,62] impose a sparseness condition, $S(E) \lesssim 2\pi[E + (c/12)]$ for $-(c/12) \leq E \leq (c/12)$, with $c = 6N^2$ for $D1-D5$ CFT_2. The SO(3) branch lies well below this bound (see dot-dashed brown curve in Fig. 2). Solutions approaching the bound might require localization on T^4, generalizing our translationally invariant solutions [63]. This would solve the puzzle raised by the CFT sparseness bound. Solutions breaking more S^3 symmetries likely have lower entropy.

Computing entanglement entropy S_{EE} and other observables for SO(3) black holes would test conjectures from [7]. There, $U(1)^2$ and BTZ $\times S^3 \times T^4$ phases have similar S_{EE} at small energies due to an "entanglement shadow" where the Ryu-Takayanagi surface [64,65] cannot probe infrared differences [66–68]. SO(3) solutions, with distinct horizon topology, may deviate from this universal behavior and could provide nontrivial tests of the eigenstate thermalization hypothesis [69,70], including examples of quantum scars [71,72]. They also provide a platform to apply novel methods for computing entanglement in solutions with nontrivial internal dependence [7]. Finally, BTZ $\times S^3 \times T^4$ is the near-horizon limit of the $D1$-$D5$-P black hole. AdS/CFT reproduces its microscopic entropy [73], and asymptotically $AdS_3 \times S^3 \times T^4$ solutions are central to the fuzz ball program [74–76]. Understanding the thermodynamics and microscopic description of SO(3) localized black holes could provide valuable insights into this framework.

Acknowledgments—We are grateful to Iosif Bena and Pierre Heidmann for their valuable comments on an earlier draft and for stimulating discussions that enriched our results. O. J. C. D. acknowledges financial support from the STFC "Particle Physics Grants Panel (PPGP) 2020" Grant No. ST/X000583/1. J. E. S. has been partially supported by STFC consolidated Grant No. ST/X000664/1. J. E. S. would also like to thank the Simons Center for Geometry and Physics for its hospitality, where this work was completed. The authors acknowledge the use of the IRIDIS High Performance Computing Facility, and associated support services at the University of Southampton, in the completion of this work.

Data availability—The data that support the findings of this article are openly available [77].

[1] J. M. Maldacena, Int. J. Theor. Phys. **38**, 1113 (1999) [Adv. Theor. Math. Phys. **2**, 231 (1998)].
[2] S. S. Gubser, I. R. Klebanov, and A. M. Polyakov, Phys. Lett. B **428**, 105 (1998).
[3] E. Witten, Adv. Theor. Math. Phys. **2**, 253 (1998).
[4] J. R. David, G. Mandal, and S. R. Wadia, Phys. Rep. **369**, 549 (2002).
[5] L. Eberhardt, M. R. Gaberdiel, and R. Gopakumar, J. High Energy Phys. 02 (2020) 136.
[6] We consider the low-energy limit with $N \to \infty$ and large 't Hooft coupling.
[7] I. Bena, R. Dulac, P. Heidmann, and Z. Wei, J. High Energy Phys. 10 (2025) 165.
[8] These solutions were first constructed in [9], and were recently analyzed in [10].
[9] I. Bah and P. Heidmann, J. High Energy Phys. 02 (2023) 133.
[10] J.-i. Sakamoto and S. Tomizawa, J. High Energy Phys. 12 (2025) 049.
[11] Although the topology is the same in both cases, the geometry of the S^3 differs significantly. For the BTZ black hole, the S^3 is simply the standard round sphere, whereas for the black poles the S^3 incorporates the asymptotic S^1 contained within global AdS_3.
[12] O. J. C. Dias, J. E. Santos, and B. Way, J. High Energy Phys. 04 (2015) 060.
[13] O. J. C. Dias, J. E. Santos, and B. Way, Phys. Rev. Lett. **117**, 151101 (2016).
[14] O. J. C. Dias, J. E. Santos, and B. Way, J. High Energy Phys. 06 (2017) 029.
[15] O. J. C. Dias and J. E. Santos, Phys. Rev. Lett. **134**, 231402 (2025).
[16] R. Gregory and R. Laflamme, Phys. Rev. Lett. **70**, 2837 (1993).
[17] T. Harmark and N. A. Obers, J. High Energy Phys. 05 (2002) 032.
[18] B. Kol, J. High Energy Phys. 10 (2005) 049.

[19] H. Kudoh and T. Wiseman, Phys. Rev. Lett. **94**, 161102 (2005).
[20] T. Harmark, V. Niarchos, and N. A. Obers, Classical Quantum Gravity **24**, R1 (2007).
[21] M. Headrick, S. Kitchen, and T. Wiseman, Classical Quantum Gravity **27**, 035002 (2010).
[22] O. J. C. Dias, J. E. Santos, and B. Way, Classical Quantum Gravity **33**, 133001 (2016).
[23] S. G. Avery, Ph.D. thesis, The Ohio State University, 2010.
[24] P. Figueras, J. Lucietti, and T. Wiseman, Classical Quantum Gravity **28**, 215018 (2011).
[25] See Supplemental Material at http://link.aps.org/supplemental/10.1103/f2rs-p1mq for details of the equations of motion, boundary conditions, numerical method, thermodynamic quantities and additional figures.
[26] Our reference metric limits $\rho_0 < \pi$, but our solutions are well within this bound.
[27] I. Kanitscheider, K. Skenderis, and M. Taylor, J. High Energy Phys. 04 (2007) 023.
[28] I. Kanitscheider, K. Skenderis, and M. Taylor, J. High Energy Phys. 06 (2007) 056.
[29] K. Skenderis and M. Taylor, J. High Energy Phys. 05 (2006) 057.
[30] H. Kim, L. Romans, and P. van Nieuwenhuizen, Phys. Rev. D **32**, 389 (1985).
[31] M. Gunaydin and N. Marcus, Classical Quantum Gravity **2**, L11 (1985).
[32] S. Lee, S. Minwalla, M. Rangamani, and N. Seiberg, Adv. Theor. Math. Phys. **2**, 697 (1998).
[33] S. Lee, Nucl. Phys. **B563**, 349 (1999).
[34] G. Arutyunov and S. Frolov, Phys. Rev. D **61**, 064009 (2000).
[35] K. Skenderis and M. Taylor, J. High Energy Phys. 08 (2006) 001.
[36] K. Skenderis and M. Taylor, J. High Energy Phys. 09 (2007) 019.
[37] R. M. Wald, Phys. Rev. D **48**, R3427 (1993).
[38] V. Iyer and R. M. Wald, Phys. Rev. D **50**, 846 (1994).
[39] V. Iyer and R. M. Wald, Phys. Rev. D **52**, 4430 (1995).
[40] R. M. Wald and A. Zoupas, Phys. Rev. D **61**, 084027 (2000).
[41] I. Papadimitriou and K. Skenderis, J. High Energy Phys. 08 (2005) 004.
[42] O. J. C. Dias, G. S. Hartnett, and J. E. Santos, Classical Quantum Gravity **38**, 015003 (2021).
[43] V. E. Hubeny and M. Rangamani, J. High Energy Phys. 05 (2002) 027.
[44] A. Buchel and L. Lehner, Classical Quantum Gravity **32**, 145003 (2015).
[45] P. Bosch, A. Buchel, and L. Lehner, J. High Energy Phys. 07 (2017) 135.
[46] S. Hawking and D. N. Page, Commun. Math. Phys. **87**, 577 (1983).
[47] E. Witten, Adv. Theor. Math. Phys. **2**, 505 (1998).
[48] S. Catterall and T. Wiseman, J. High Energy Phys. 12 (2007) 104.
[49] K. N. Anagnostopoulos, M. Hanada, J. Nishimura, and S. Takeuchi, Phys. Rev. Lett. **100**, 021601 (2008).
[50] S. Catterall and T. Wiseman, Phys. Rev. D **78**, 041502 (2008).
[51] M. Hanada, Y. Hyakutake, J. Nishimura, and S. Takeuchi, Phys. Rev. Lett. **102**, 191602 (2009).
[52] S. Catterall and T. Wiseman, J. High Energy Phys. 04 (2010) 077.
[53] M. Hanada, J. Nishimura, Y. Sekino, and T. Yoneya, J. High Energy Phys. 12 (2011) 020.
[54] M. Hanada, Y. Hyakutake, G. Ishiki, and J. Nishimura, Science **344**, 882 (2014).
[55] B. A. Berg and T. Neuhaus, Phys. Rev. Lett. **68**, 9 (1992).
[56] J. Lee, Phys. Rev. Lett. **71**, 211 (1993).
[57] F. Wang and D. P. Landau, Phys. Rev. E **64**, 056101 (2001).
[58] G. T. Horowitz, in *Workshop on Conference on the Future of Theoretical Physics and Cosmology in Honor of Steven Hawking's 60th Birthday* (Cambridge University Press, Cambridge, 2002), pp. 310–329.
[59] T. Harmark and N. A. Obers, Nucl. Phys. **B684**, 183 (2004).
[60] T. Harmark, Phys. Rev. D **69**, 104015 (2004).
[61] O. J. Dias, T. Harmark, R. C. Myers, and N. A. Obers, Phys. Rev. D **76**, 104025 (2007).
[62] T. Hartman, C. A. Keller, and B. Stoica, J. High Energy Phys. 09 (2014) 118.
[63] O. J. C. Dias, J. E. Santos, and B. Way, J. High Energy Phys. 05 (2018) 111.
[64] S. Ryu and T. Takayanagi, Phys. Rev. Lett. **96**, 181602 (2006).
[65] V. E. Hubeny, M. Rangamani, and T. Takayanagi, J. High Energy Phys. 07 (2007) 062.
[66] V. Balasubramanian, B. D. Chowdhury, B. Czech, and J. de Boer, J. High Energy Phys. 01 (2015) 048.
[67] J. Caminiti, B. Friedman-Shaw, A. May, R. C. Myers, and O. Papadoulaki, J. High Energy Phys. 10 (2024) 119.
[68] G. Arora, M. Headrick, A. Lawrence, M. Sasieta, and C. Wolfe, SciPost Phys. **16**, 152 (2024).
[69] M. Srednicki, Phys. Rev. E **50**, 888 (1994).
[70] J. M. Deutsch, Phys. Rev. A **43**, 2046 (1991).
[71] H. Bernien *et al.*, Nature (London) **551**, 579 (2017).
[72] C. J. Turner, A. A. Michailidis, D. A. Abanin, M. Serbyn, and Z. Papić, Nat. Phys. **14**, 745 (2018).
[73] A. Strominger and C. Vafa, Phys. Lett. B **379**, 99 (1996).
[74] S. D. Mathur, Fortschr. Phys. **53**, 793 (2005).
[75] K. Skenderis and M. Taylor, Phys. Rep. **467**, 117 (2008).
[76] S. D. Mathur and M. Mehta, arXiv:2412.09495.
[77] J. C. Dias Oscar and E. Santos Jorge, Localised $AdS_3 \times S^3 \times \mathbb{T}^4$ Black Holes, arXiv:2508.16722.